Reconfigurable Fractional-Order Filter with Electronically Controllable Slope of Attenuation, Pole Frequency and Type of Approximation

JEŘÁBEK, J.; ŠOTNER, R.; DVOŘÁK, J.; POLÁK, J.; KUBÁNEK, D.; HERENCSÁR, N.; KOTON, J.

Accepted manuscript

World Scientific
www.worldscientific.com

Reconfigurable Fractional-Order Filter with Electronically Controllable Slope of Attenuation, Pole Frequency and Type of Approximation

Jan Jerabek[*], Roman Sotner, Jan Dvorak, Josef Polak, David Kubanek, Norbert Herencsar and Jaroslav Koton

Department of Telecommunications, Brno University of Technology, Technicka 12,
Brno, 616 00, Czech Republic[*]
jerabekj@feec.vutbr.cz
sotner@feec.vutbr.cz
dvorakjan@phd.feec.vutbr.cz
xpolak24@phd.feec.vutbr.cz
kubanek@feec.vutbr.cz
herencsn@feec.vutbr.cz
koton@feec.vutbr.cz

This paper presents design of electronically reconfigurable fractional-order filter that is able to be configured to operate as fractional-order low-pass filter (FLPF) or fractional-order high-pass filter (FHPF). Its slope of attenuation between pass band and stop band, i.e. order of the filter, is electronically adjustable in range between 1 and 2. Also pole frequency can be electronically controlled independently with respect to other tuned parameters. Moreover, particular type of approximation can be also controlled electronically. This feature set is available both for FLPF and FHPF type of response. Presented structure of the filter is based on well-known follow-the-leader feedback (FLF) topology adjusted in our case for utilization with just simple active elements operational transconductance amplifiers (OTAs) and adjustable current amplifiers (ACAs), both providing possibility to control its key parameter electronically. Paper explains how reconfigurable 3rd-order FLF topology is used in order to approximate both FLPF and FHPF in concerned frequency band of interest. Design is supported by PSpice simulations for three particular values of order of the filter (1.25, 1.5, 1.75), for several values of pole frequency and for two particular types of approximation forming the shape of both the magnitude and phase response. Moreover, theoretical presumptions are successfully confirmed by laboratory measurements with prepared prototype based on behavioral modeling.

Keywords: adjustable current amplifier; approximation; ACA; fractional-order filter; fractional-order high-pass filter; fractional-order low-pass filter; FLF; follow-the-leader feedback; fractional order; operational transconductance amplifier; OTA; reconfigurable filter.

1. Introduction

Each analog circuit needs passive elements (resistors, capacitors, inductors in most cases). These passive elements are used for further synthesis together with active elements to create linear (integrators, amplifiers, …) and nonlinear (comparators, shapers, switches, …) functional blocks. Finally, these blocks create simple or complex applications (filters,

---

[*] Corresponding author.

oscillators, generators, modulators, mixers, …) that are implemented in complex mixed (analog and digital) systems (transceivers, systems for sensor processing, measuring devices, systems for communication, etc.). Common approaches in synthesis and design of linear circuits suppose integer order of the used passive reactive components and integer order of resulting functional block (and application). This fact results from character of commonly available (on the market) passive elements. Integer-order passive elements are currently easily producible because of technological aspects.

However, in some cases, also fractional-order systems[1-3] are important due to their ability to describe real-world processes and phenomena. Many systems in nature have rather fractional character and nonlinear behavior that differs from their common linear and integer-order approximations used for better understanding and simpler modeling. Typical examples can be found in many analog systems for signal processing (filters, amplifiers, controllers, immittance circuits, etc.). For instance, we can mention modeling of impedance[4] of biological tissue[5] that is typical example of fractional-order behavior. The impedance characteristic of this biological matter can be modeled by fractional-order model where fractional-order passive elements are required.

There are two possibilities how to synthetize the fractional-order immittance elements. We can use standard synthesis when passive elements (capacitors in many cases) are directly replaced by elements with fractional character. There are several methods how to construct these elements[6-8] (RC ladder structures and chains in the most cases). They are referred to as approximants because resulting two-terminal device provides only approximation of requested frequency characteristic (immittance) in limited frequency band and with certain phase ripple. These features depend on selected approximation, usually having polynomial character. There are even attempts to use only appropriate locations of zeros and poles of the immittance or transfer function (in case of two-port system) instead of any mathematical approximation (implemented in Mathcad[9]). These locations of poles and zeros frequencies can be also achieved quite simply by PSpice Optimizer tool for example[10-12].

The second method supposes synthesis of special replacement of fractional-order passive element (fractional-order capacitor in most cases) that is applied in original structure of the designed fractional-order systems. However, increased circuit complexity, power consumption, influences of real parasitic features of used active elements necessary for these solutions are substantial in many cases. Typical examples of this method are given in[13,14]. Note that fractional behavior of the two terminal system can be obtained as output response of the active filter of high-integer-order with appropriate setting of values of transfer coefficients (so-called continuous fraction expansion) supplemented with simple conversion of output signal into the input node[14-16]. Accuracy of the immittance is given by mathematical approximation used in such filter[17,18] and by coefficients and order of the filter[19,20]. We can also use direct synthesis of the "active" immittance from required locations of zeros and poles[21]. This method is not using special polynomial mathematical approximations noted above. Required bandwidth of resulting approximant and corresponding phase ripple determines locations and number of these roots directly. This

method leads to chains of many sub-block (so-called bilinear sections/immittances with independently adjustable poles and zeros[21]). Bilinear two-ports (building blocks, e.g. integrator) also exists[11,22]. The required phase ripple and bandwidth of validity of approximation determine the minimal number of necessary sections.

Note that real fractional-order devices (two-terminal systems) are developed and studied also as solid-state devices based on some chemical/technological mixtures, see for example to Ref. 23 - 25. There are also the very first attempts to prepare passive element having fractional-order features on chip[26], however inventors are contending several issues and presented implementation has several drawbacks.

Usefulness of the fractional-order filters lays in possibility to set theoretically arbitrary slope of its magnitude response and also theoretically arbitrary maximal phase shift. Classic integer-order filters have steepness between pass and stop band given by $20 \cdot n$ dB/dec where n is nonzero integer value ($90° \cdot n$ for maximal phase shift in phase response) and depends significantly on number of independent accumulation elements (capacitor, inductors) present in the filtering structure. Fractional-order circuits (basic two-terminals and two ports, i.e. immittances, integrators, differentiators) generally have arbitrary slope of magnitude response ($20 \cdot a$ dB/dec) and maximal phase shift ($90° \cdot a$)[11], where $a > 0$ and a is real number. However, this approach is not common because of its impracticality. General frequency response of the fractional-order filter is therefore frequently described by magnitude slope $20 \cdot (n+a)$ dB/dec and phase shift $90° \cdot (n+a)$ as combination of integer and fractional part/contribution in filters with order higher than 1 ($n \geq 1$ and $0 < a < 1$). Note that a is also very often referred to as α.

As already discussed, except investigation of solutions of fractional-order replacements (approximants) of "passive" elements (typical examples of single-purpose filters are given in Ref. 13, Ref. 27-30), there are also methods how to design directly two-port systems (filters in many cases[17,18] for example) without fractional-order passive elements or their active replacements[31-35]. Some of these works relevant for purposes of this paper are summarized in the following Table 1. Almost all of these circuits are designed for operation in low-frequency bands (up to units or tens of kHz). Except solutions presented in Ref. 34, key features, like reconfigurability of the transfer function, control of pole frequency as well as control of the order of the filter are not present in frame of one designed structure, and these solutions are not providing this mutually independent and electronical type of control at the same time.

This work focuses on the design of fractional-order filter without fractional-order passive elements or their active replacements. Filter provides electronical reconfigurability between fractional-order low-pass filter (FLPF) and fractional-order high-pass filter (FHPF). Pole frequency and also order of the filter are electronically controlled by parameters and coefficients of the filter in both configurations (FLPF and FHPF). Moreover, type of the fractional-order approximation can be also controlled electronically, because all relevant parameters of integer-order transfer function can be controlled electronically. Design is supported not only by simulations, but also by experimental

laboratory measurements. Our secondary goal was also to compare two particular and most frequently used types of fractional-order approximations as described below.

The text is organized as follows. After introductory part explaining our motivation and providing state of the art, brief overview about relevant active elements is given. Next chapter focuses on details about two common approximations and the design of the FLF topology suitable for fulfilling requirements on electronically controllable and reconfigurable fractional-order filter that is presented together with numerical design in chapter 4. Chapter 5 includes comparison of simulation and measurement results for several scenarios. This chapter gives very complex overview of behavior of the filter under particular circumstances. The last chapter summarizes the most significant findings of this paper.

2. Active Elements

The designed filter, presented in the following chapter contains two basic types of controllable active elements. First one is well-known Operational Transconductance Amplifier (OTA)[36] with current outputs (Fig. 1). Second one is the single-input Adjustable Current Amplifier[37] (with adjustable current gain) also with several current outputs (Fig. 2).
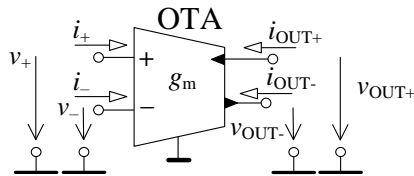

Fig. 1. Operational Transconductance Amplifier (OTA) schematic symbol (dual-output version).

Standard operation of OTA in dual-output configuration as shown in Fig. 1 is described by these straightforward equations:

$$i_{OUT+} = -i_{OUT-} = g_m(v_+ - v_-) \ . \tag{1}$$

Note that transconductance parameter (g_m) is usually controlled by external DC current and therefore OTA can be considered as simple electronically controllable active element.

Normal operation of ACA is also very simple

$$i_{OUT+} = -i_{OUT-} = B \cdot i_{IN} \ . \tag{2}$$

Current gain (B) is also usually controlled externally, in many cases by DC voltage (referred to as V_{SET_B} in the following Fig. 2).

Table 1. Comparison of features of the most relevant previously reported fractional-order filters without fractional-order passive elements or their active replacements.

Reference	Type of active elements (number)	Type of passive elements (number)	Order of the integer-order filter	Transfer function type(s)	Topology	Simulated (sim) / Measured (meas)	Multi-functional / Reconfigurable	Tested values of $(n+a)$ or a or $a_1 + a_2$	Electronic control-lability	Controlled by value of
[17]	9 to 12[a]	C (3)	3	LP or HP	FLF	sim	No	1.3, 1.5, 1.7	Yes	g_m
[18]	(3)[b]	C (3)	3	LP	FLF	sim	No	1.3, 1.5, 1.7	Yes	R_X and C
[31]	OA (2)	C (3), R (10)	3	LP	N/A	sim / meas	No	1.1, 1.5, 1.9	No	R
[32]	OA (10)	C (7)	7	LP, HP, BR	FLF	sim / meas	Not tested	5.1, 5.3, 5.5, 5.7, 5.9	No	R
[33][c]	DDCC (5)	C (3), R (7)	3	LP	IFLF	sim / meas	Not tested	1.3, 1.5, 1.7	No	R and C
[33][c]	DDCC (9)	C (7), R (11)	7	LP	IFLF, FLF	sim / meas	No	5.5	No	R and C
[34][d]	OTA (7)	C (2)	2	LP, HP, AP, BP	IFLF	sim	Yes	0.5	Yes	g_m
[34][d]	OTA (11)	C (4)	4	LP, HP, BR, BP	IFLF	sim	Yes	1+0.5, 0.7+0.5, 0.8+0.7, 0.9+0.9	Yes	g_m
[35]	CF (5), ACA (5)	C (3), R (3)	3	LP	FLF	sim	No	1.2, 1.5, 1.8	Yes	B
proposed	OTA (3), CF (2), ACA (3)	C (3)	3	LP, HP	FLF	sim / meas	Yes	1.25, 1.5, 1.75	Yes	g_m, B

[a]Three slightly different solutions presented in one paper having various types of active elements and providing different types of response.

[b]Three integrators in CMOS.

[c]One reseach paper presenting two solutions.

[d]Two variants within one research paper.

Previously unexplained abbreviations: OA – operational amplifier, DDCC – differential difference current conveyor, OTA – operational transconductance amplifier, CF – current follower, ACA – adjustable current amplifier, g_m – transconductance, B – current gain, BR – band reject, AP – all pass.
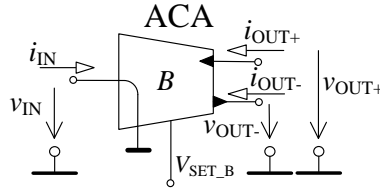
Fig. 2. Adjustable Current Amplifier (ACA) schematic symbol (dual-output version).

Note that for current gain fixed to 1 or −1, this element is frequently referred to as Current Follower (CF) in case of having single output. If there are two current outputs, element is known as Dual-Output CF (DO-CF)[37], usually with two opposite polarities of output currents having same magnitude value. Description of the DO-CF element is because of its simplicity omitted in this paper. However, it should be noted that two DO-CF-s are required in the design of the reconfigurable fractional-order filter.

3. Proposal of the reconfigurable fractional-order filter

This chapter describes design procedure of the reconfigurable fractional-order filter. First subsection is about design of FLPF, second about FHPF and third part is about its linking into one reconfigurable solution.

3.1. *Butterworth approximation of the fractional-order low-pass filter*

Design procedure of the fractional-order low-pass filter (FLPF) having order of $(1 + a)$ was precisely described in Ref. 19 and also Ref. 17. Starting transfer function is in the following form:

$$K_{1+a}^{LP}(s) = \frac{K_1}{s^{1+a} + s^a K_3 + K_2} \quad .$$
(3)

where from Ref. 17:

$$
\begin{aligned}
K_1 &= 1 \; , \\
K_2 &= 0.2937\,a + 0.71216 \; , \\
K_3 &= 1.068\,a^2 + 0.161a + 0.3324 \; .
\end{aligned}
$$
(4)

Coefficients K_X, where $X = 1, 2, 3$ influence directly the shape of the obtained transfer characteristic. Note that the values of K_X are dependent on the parameter a, i.e. on the order of the filter. Second-order approximation of s^a term from eq. 3 is given by:

$$s^a = \frac{a_0 s^2 + a_1 s + a_2}{a_2 s^2 + a_1 s + a_0} \quad .$$
(5)

There are several ways how to approximate coefficients a_0, a_1 and a_2 from eq. 5 and two of them are going to be compared within this paper. First set of coefficients can be calculated as follows[32]:

$$a_0 = 2(1 + a) \ ,$$
$$a_1 = 5 - a^2 \ ,$$
$$a_2 = 2(1 - a) \ .$$

(6)

Second approximation[19] is defined by

$$a_0 = a^2 + 3a + 2 \ ,$$
$$a_1 = 8 - 2a^2 \ ,$$
$$a_2 = a^2 - 3a + 2 \ .$$

(7)

Note that these approximations are going to be referred to as 1st and 2nd approximation in the rest of the text.

The following standard 3rd-order transfer function will be used to emulate FLPF with Butterworth approximation of order $(1 + a)$ [17]:

$$K_{1+a}^{LP}(s) \cong \frac{K_1}{a_0} \frac{s^2 a_2 + s a_1 + a_0}{s^3 + s^2 b_2 + s b_1 + b_0} \ .$$

(8)

Formulas for a_X coefficients are shown above (two possible approximations), b_X coefficients (where $X = 0, 1, 2$) are taken from Ref. 19:

$$b_0 = \frac{a_0 K_2 + a_2 K_3}{a_0} \ ,$$
$$b_1 = \frac{a_1 (K_2 + K_3) + a_2}{a_0} \ ,$$
$$b_2 = \frac{a_1 + a_0 K_3 + a_2 K_2}{a_0} \ .$$

(9)

Again, it is worth mentioning that these coefficients are all dependent on parameter a. One of possible ways how to implement 3rd-order transfer function is to use follow the leader (FLF) filtering topology. Fig. 3 shows the possible block diagram[48], consisting in our case of three inverting integrators, three feedback loops and three forward signal paths. Note that this topology is going to be used for the filter design below. General transfer function of this topology can be derived directly from Fig. 3 and it is

$$K(s) = \frac{I_{OUT}}{I_{IN}} = \frac{s^2 \dfrac{G_1}{\tau_1} + s \dfrac{G_2}{\tau_1 \tau_2} + \dfrac{G_3}{\tau_1 \tau_2 \tau_3}}{s^3 + s^2 \dfrac{1}{\tau_1} + s \dfrac{1}{\tau_1 \tau_2} + \dfrac{1}{\tau_1 \tau_2 \tau_3}} \quad . \tag{10}$$
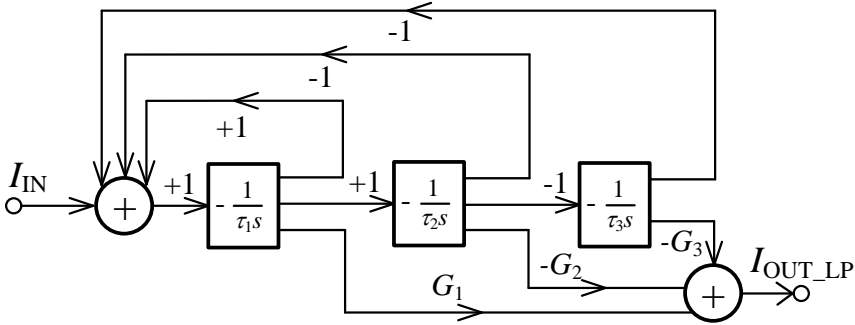

Fig. 3. Block diagram of a FLF (follow-the-leader feedback) topology[48] used for approximation of the FLPF (fractional-order low-pass filter) of $(1 + a)$ order.

Set of equations how to obtain τ_X and G_X (when $X = 1, 2, 3$) in eq. 10 from a_X and b_X coefficients (where $X = 1, 2, 3$) are obvious when comparing eq. 10 and eq. 8.

3.2. *Butterworth approximation of the fractional-order high-pass filter*

Similarly to FLPF, design procedure of the fractional-order high-pass filter (FHPF) having order of $(1 + a)$ was also precisely described in Ref. 17. Starting transfer function is in the following form:

$$K_{1+a}^{HP}(s) = \frac{K_1 s^{1+a}}{K_2 s^{1+a} + K_3 s^a + 1} \quad , \tag{11}$$

where coefficients K_X, $(X = 1, 2, 3)$, are defined exactly the same way as in case of FLPF, i.e. by eq. 4. Similarly, eqs. 5 to 7 also apply for FHPF design procedure.

Based on this, the following standard 3rd-order transfer function will be used to emulate FHPF with Butterworth approximation of order $(1 + a)$[17]:

$$K_{1+a}^{HP}(s) \cong \frac{K_1}{a_0} \frac{a_0 s^3 + a_1 s^2 + s a_2}{s^3 + \dfrac{b_1}{b_0} s^2 + \dfrac{b_2}{b_0} s + \dfrac{1}{b_0}} \quad . \tag{12}$$

Formulas for a_X coefficients are shown above in two possible approximations (eq. 6, eq. 7), b_X coefficients are equal to eq. 9 shown above.

In this particular case, 3rd-order transfer function based of FLF type of topology can be also used. Fig. 4 shows the particular block diagram[49], consisting of inverting integrators, supplemented by three feedback loops and three forward signal paths. Transfer function of this general topology is

$$K(s) = \frac{\boldsymbol{I}_{OUT}}{\boldsymbol{I}_{IN}} = \frac{s^3 G_1 + s^2 \dfrac{G_2}{\tau_1} + s \dfrac{G_3}{\tau_1 \tau_2}}{s^3 + s^2 \dfrac{1}{\tau_1} + s \dfrac{1}{\tau_1 \tau_2} + \dfrac{1}{\tau_1 \tau_2 \tau_3}} \cdot \tag{13}$$

Similarly to FLPF, equations how to obtain τ_X and G_X from a_X and b_X coefficients are obvious when comparing eq. 13 and eq. 12.
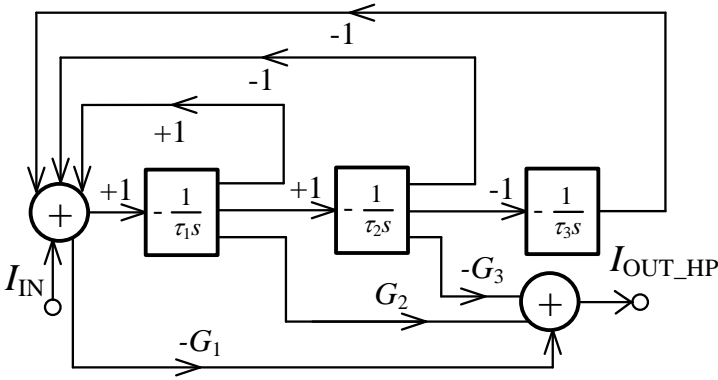

Fig. 4. Block diagram of a 3rd-order FLF (follow-the-leader feedback) topology[49] used for approximation of the FHPF (fractional-order high-pass filter) of $(1 + a)$ order.

3.3. *Linking of FLPF and FHPF topology into one structure*

When we compare Fig. 3 and Fig. 4, it is clear that these topologies are very similar. Therefore, these topologies could be linked together and actually made by one general FLF structure with just two additional switches referred to as "LP" and "HP" in the following Fig. 5 showing final form of the block diagram of designed reconfigurable fractional-order filter. These switches could be implemented easily by additional transistor-level structures or additional ACA active elements providing zero or unity gain in particular forward branch of this current-mode circuit.
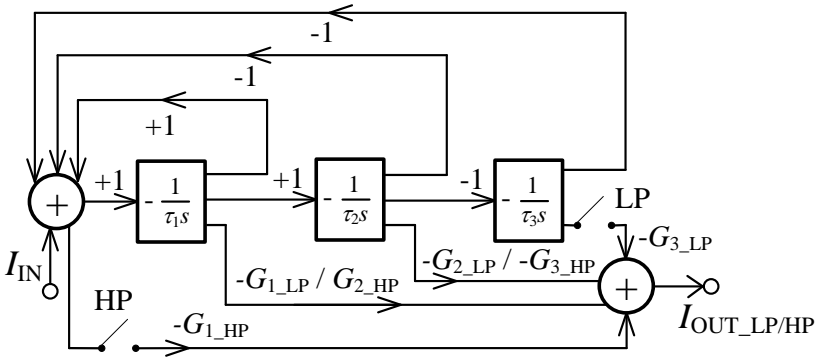
Fig. 5. Generalized block diagram of a 3rd-order FLF (follow-the-leader feedback) topology used for approximation of both the FLPF and FHPF of $(1 + a)$ order.

Designed reconfigurable filter with active elements introduced in chapter 2 and based on generalized FLF block topology (Fig. 5) is shown in Fig. 6. It is obvious that there are three OTA amplifiers with g_{m1}, g_{m2} and g_{m3} controllable parameters, three ACA elements having B_1, B_2 and B_3 gains and two supplementary DO-CF-s. One of them is near input of the filter, the second one is not shown directly in Fig. 6. However, it forms part of DO-ACA1, because this element is actually built by ACA and DO-CF element as will be described below. There are also three capacitors, in each case at the input high-impedance terminal of OTA element, in order to form inverting lossless integrator as shown in generalized block structure (Fig. 5).
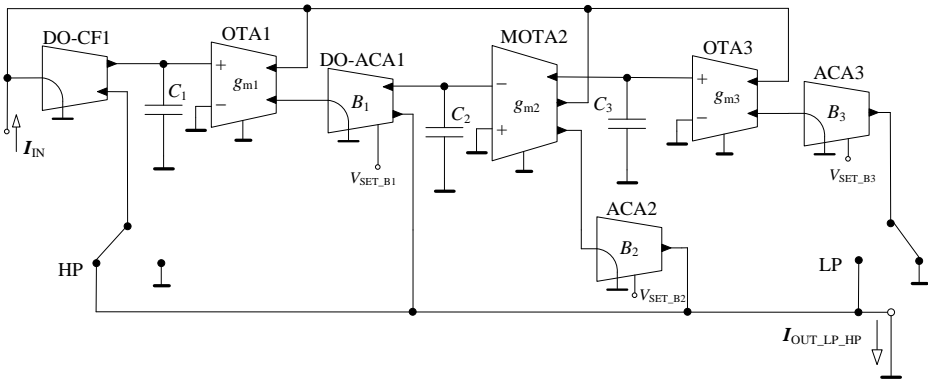

Fig. 6. Particular solution of reconfigurable 3rd-order FLF (follow-the-leader feedback) topology used for approximation of both the FLPF and FHPF of $(1 + a)$ order. Currently in HP response configuration shown as an example.

Generally, transfer function of filter from Fig. 6 is:

$$K_{general}(s) = \frac{I_{OUT\_LP\_HP}}{I_{IN}} = \frac{N_{LP\_or\_HP}(s)}{D_{general}(s)} \quad . \tag{14}$$

Denominator of this transfer function is equal to:

$$D_{general}(s) = s^3 + s^2 \frac{g_{m1}}{C_1} + s \frac{g_{m1}g_{m2}B_1}{C_1C_2} + \frac{g_{m1}g_{m2}g_{m3}B_1}{C_1C_2C_3} \quad . \tag{15}$$

If "LP" switch is "on" and "HP" switch is "off", FLPF response is configured from the general filtering structure and nominator is as follows:

$$N_{LP}(s) = -s^2 \frac{g_{m1}B_1}{C_1} - s \frac{g_{m1}g_{m2}B_1B_2}{C_1C_2} - \frac{g_{m1}g_{m2}g_{m3}B_1B_3}{C_1C_2C_3} \quad . \tag{16}$$

If "LP" switch is "off" and "HP" switch is "on", FHPF response is configured and nominator is in the following form:

$$N_{HP}(s) = -s^3 - s^2 \frac{g_{m1}B_1}{C_1} - s \frac{g_{m1}g_{m2}B_1B_2}{C_1C_2} \quad . \tag{17}$$

It is obvious that both eq. 16 and eq. 17 together with eq. 15 represent inverting form of the transfer function and reconfiguration of the type of transfer function is available by control of "LP" and "HP" switches. Particular meaning of quantities or variables used in eqs. 15, 16 and 17 is obvious from Fig. 6. As already mentioned, several parameters can be controlled electronically (all values except values of C_1, C_2 and C_3), which is beneficial feature for future change of the filter order and also the control of the pole frequency. This is going to be demonstrated in the following sections.

4. Numerical design of the reconfigurable filter

4.1. *FLPF mode of reconfigurable filter*

In order to verify the design, values of all components have been calculated based on eqs. 3 to 10 and eqs. 14 to 16. Chosen parameters of the filter are: starting pole frequencies determining the pass-band: $f_{0\_LP} = \omega_0/2\pi = 100$ kHz, values of capacitors: $C_1 = 1.8$ nF, $C_2 = 470$ pF and $C_3 = 18$ nF. The rest of the parameters is dependent on chosen type of approximation of s^a term, i.e. eqs. 6 and 7. Calculated values for 1st / 2nd approximation are summarized in Table 2.

Table 2. Numerical values of relevant parameters of the filter in FLPF configuration for $f_{0\_LP} = 100$ kHz. Both 1st and 2nd approximation (1st/2nd value if applicable).

	Order of the filter		
Particular parameter	1.25	1.5	1.75
C_1 [nF]	1.8	1.8	1.8
C_2 [pF]	470	470	470
C_3 [nF]	18	18	18
$R_1 = 1/g_{m1}$ [Ω]	306 / 245	347 / 310	360 / 348
$R_2 = 1/g_{m2}$ [Ω]	673 / 406	408 / 207	182 / 76
$R_3 = 1/g_{m3}$ [Ω]	254 / 348	226 / 291	217 / 256
B_1 [-]	0.208 / 0.129	0.131 / 0.075	0.058 / 0.026
B_2 [-]	0.654 / 0.719	0.572 / 0.610	0.476 / 0.492
B_3 [-]	0.953 / 1.009	0.921 / 1.005	0.923 / 0.999

4.2. *FHPF mode of reconfigurable filter*

Based on eqs. 11, 4 to 7, 9 and eqs. 13 to 15 and 17, and similarly to the FLPF design described in the previous chapter, values of all components have been calculated. Chosen parameters of the filter are exactly the same as in case of FLPF: starting pole frequencies determining the pass-band: $f_{0\_LP} = \omega_0/2\pi = 100$ kHz, values of capacitors: $C_1 = 1.8$ nF, $C_2 = 470$ pF and $C_3 = 18$ nF. This allows reconfiguration of the filter between FLPF and FHPF. The rest of the parameters is again dependent on chosen type of approximation of s^a term, i.e. eqs. 6 and 7. Calculated values for 1st / 2nd approximation are summarized in Table 3. When we compare values from Table 2 and Table 3, it is obvious that only electronically controlled parameters have to be changed during tuning of order of the filter or type of the approximation. Of course, the choice of transfer function type is done by switches "LP" and "HP", as already mentioned.

Table 3. Numerical values of relevant parameters of the filter in FHPF configuration for $f_{0\_LP} = 100$ kHz. Both 1st and 2nd approximation (1st/2nd value if applicable).

	Order of the filter		
Particular parameter	1.25	1.5	1.75
C_1 [nF]		1.8	
C_2 [pF]		470	
C_3 [nF]		18	
$R_1 = 1/g_{m1}$ [Ω]	307 / 225	347 / 268	360 / 305
$R_2 = 1/g_{m2}$ [Ω]	2432 / 2605	2283 / 2363	1894 / 1904
$R_3 = 1/g_{m3}$ [Ω]	255 / 319	225 / 252	217 / 225
B_1 [-]	0.686 / 0.712	0.621 / 0.607	0.516 / 0.493
B_2 [-]	0.218 / 0.128	0.142 / 0.070	0.063 / 0.026

4.1. *Frequency tuning of the filter*

The proposed fractional-order filter provides pole frequency control by simultaneous change of values of transconductances without disturbing quality factor and order of the filter. Chosen parameters of the capacitors and current gains are the same in case FLPF and FHPF, respectively. Order of the filter was 1.5 in each of these cases. Values of capacitors are exactly the same as in the previous case: $C_1 = 1.8$ nF, $C_2 = 470$ pF and $C_3 = 18$ nF. Calculated values of the resistors representing $1/g_m$-s of the FLPF for three selected values of the pole frequency are summarized in Table 4. Table 5 summarizes numerical values of the $1/g_m$-s for FHPF in case of the same set of pole frequencies. Note that in these tables are stated values of $1/g_m$-s for 1st / 2nd approximation.

Table 4. Numerical values of relevant parameters of the filter in FLPF configuration for constant order of the filter 1.5. Both 1st and 2nd approximation ($1^{st}/2^{nd}$ value).

	Pole frequency [kHz]		
Particular parameter	33	100	300
$R_1 = 1/g_{m1}$ [Ω]	1041 / 931	347 / 310	116 / 103
$R_2 = 1/g_{m2}$ [Ω]	1224 / 620	408 / 207	136 / 69
$R_3 = 1/g_{m3}$ [Ω]	678 / 875	226 / 291	75 / 97

Table 5. Numerical values of relevant parameters of the filter in FHPF configuration for constant order of the filter 1.5. ($1^{st}/2^{nd}$ approximation).

|	Pole frequency [kHz]		
Particular parameter	33	100	300
$R_1 = 1/g_{m1}$ [Ω]	1041 / 813	347 / 268	116 / 89
$R_2 = 1/g_{m2}$ [Ω]	6849 / 7161	2283 / 2363	761 / 788
$R_3 = 1/g_{m3}$ [Ω]	675 / 764	225 / 252	75 / 84

5. Simulation and experimental results

To verify the correct function of the proposed fractional-order topology from Fig. 6, the PSpice simulations and also experimental measurement are performed and mutually compared. The PSpice simulations of the filter were performed using behavioral simulation models of the OTA, MOTA, DO–CF and ACA elements which are mentioned in Chapter 2. For experimental measurement, the filter was implemented in PCB (Printed Circuit Board) form corresponding with the behavioral model in PSpice simulator. The OTA and MOTA elements were replaced by UCC_N1B_0520[47] chips with discrete external resistors (*R*) connected to X terminal representing g_m-s of OTA-s. The UCC_N1B_0520 chip includes one UCC (Universal Current Conveyor) active element and one second-generation Current Conveyor (CCII+/-). The DO–CF element providing input current distribution as obvious from Fig. 6, was implemented by CCII+/-. The EL2082[50] chips are

used for implementation of the ACA elements within the reconfigurable topology. Note that in order to implement dual-output version of ACA (DO-CA1 from the structure shown in Fig. 6), cascade connection of EL2082 and CCII+/- was used in case of both simulation and measurement. The current gain of the EL2082 is controlled by DC voltage in range from 0 to 2.5 V with gain numerically approximately equal to value of control voltage.

5.1. *Measurement and simulation results for FLPF*

Figure 7 illustrates measurement results (solid lines) of the electronic control of the FLPF order for 1st approximation (eq. 6) in comparison with simulation results (dashed lines). Values of all passive components and gains are summarized in Table 2. From magnitude and phase responses it is obvious that experimental results are in good agreement with simulation results, however the pole frequency from the measurement results is slightly higher in comparison with simulations. This frequency shift can be caused by inaccurate values of the used capacitors and transconductances. The biggest differences can be seen for filter with order 1.75. This difference is given mainly because value of the B_1 (see Table 2) is relatively small and therefore not enough accurate. Measurement (solid lines) and simulation (dashed lines) results of the FLPF with used approximation from eq. 7 (2nd approximation) are compared in Fig. 8. Values of all passive components and gains are also summarized in Table 2. From obtained responses it can be seen that pole frequency is slightly shifted as seen also in the previous graph. The differences between measurement and simulation results of the FLPF with order 1.75 are also caused by small value of parameters, g_{m2} and B_1 particularly.

Note that slope of attenuation of the transfer magnitude, for three selected orders and used 1st approximation, illustrated in Fig. 7, has fractional character only in short frequency range as expected because of the 2nd-order approximation of s^a, as represented by eq. 5. Slope of attenuation of the transfer functions of the filter with 2nd approximation (Fig. 8) has fractional character in wider frequency range than filter with 1st approximation. These differences are caused by type of chosen approximation. The frequency range of the fractional character is dependent on chosen value of the filter's order. Note that this applies to all achieved results in this paper.
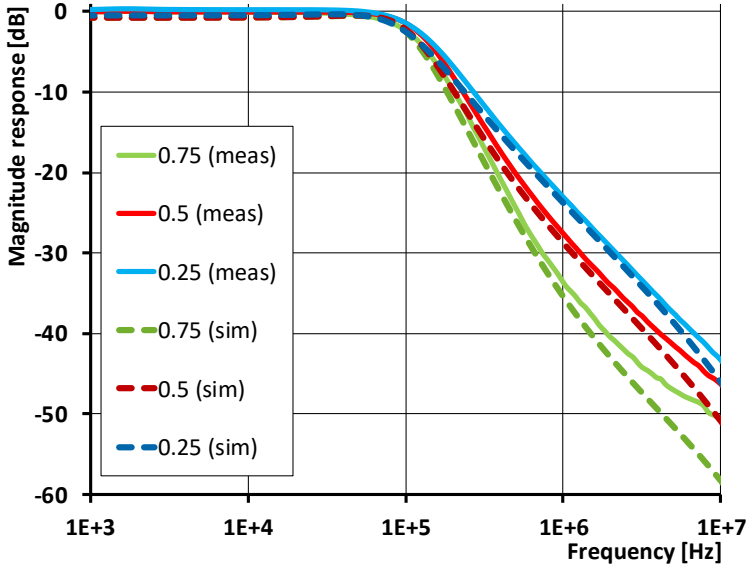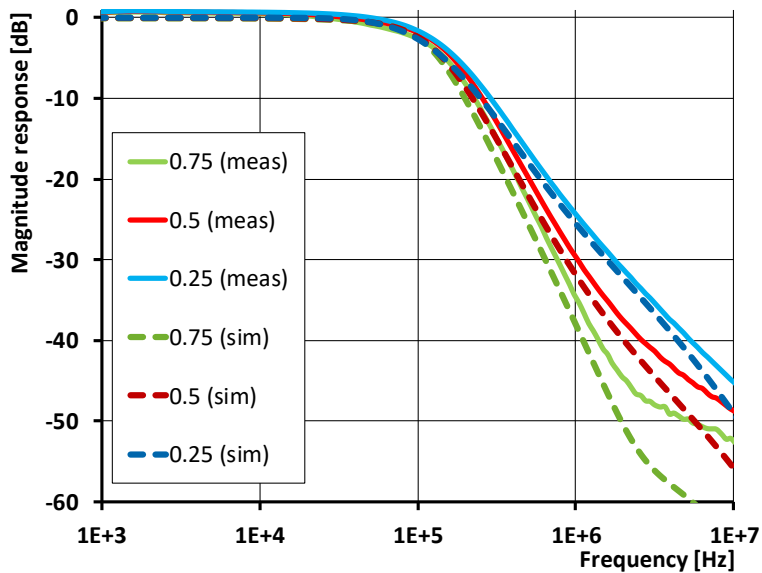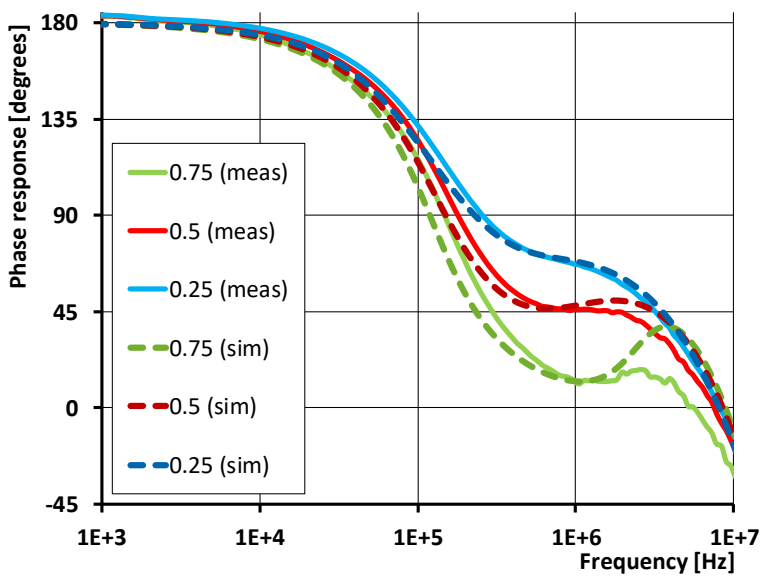
(a)
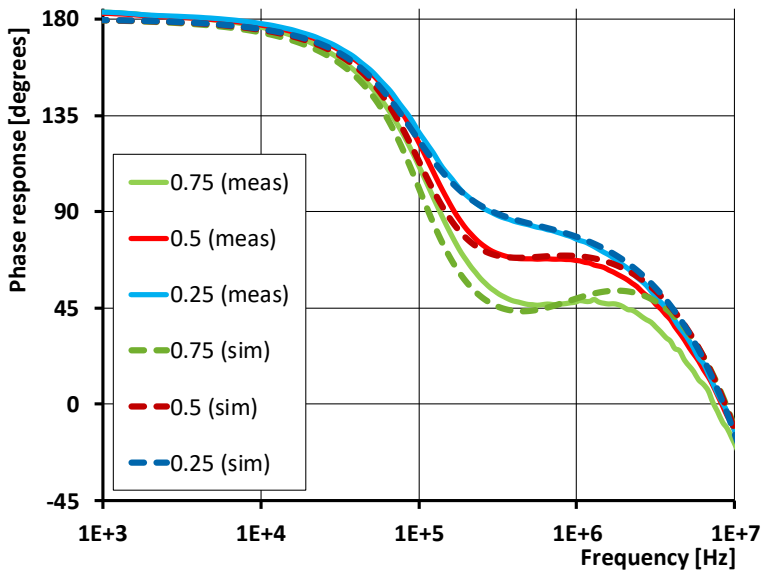
(b)

Fig. 7. Simulation (dashed lines) and measurement (solid lines) results of the FLPF for 1st approximation: (a) magnitude response, (b) phase response.
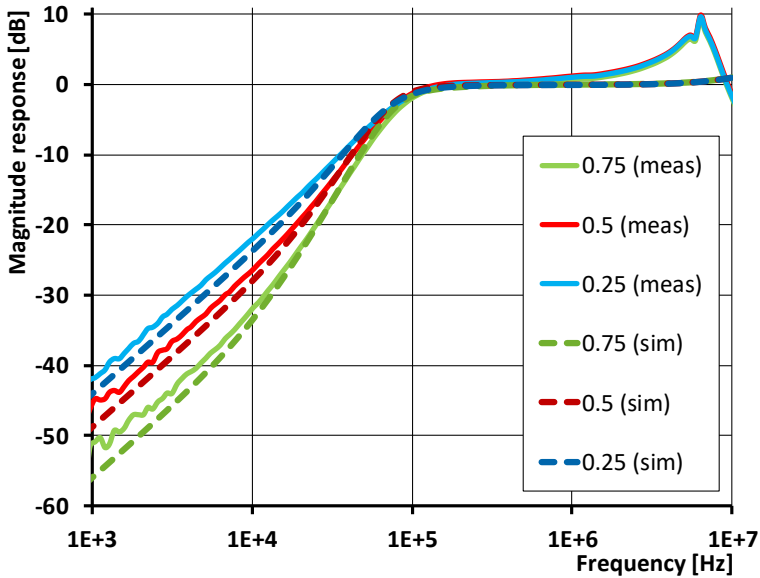
(a)

(b)

Fig. 8. Simulation (dashed lines) and measurement (solid lines) results of the FLPF for 2nd approximation: (a) magnitude response, (b) phase response.

5.2. *Measurement and simulation results for FHPF*

A comparison of the measurement and simulation results in case of electronically controlled order of the FHPF for 1st approximation based on eq. 6 is shown in Fig. 9. The chosen values of the order, when the pole frequency is 100 kHz, are the same as at the FLPF, i.e.: 1.25, 1.5 and 1.75. Values of all passive components and gains are summarized in Table 3 shown above.

Figure 10 illustrates magnitude and phase responses of the FHPF for 2nd used approximation from eq. 7. A comparison of the obtained measurement (solid lines) and simulation (dashed lines) results is demonstrated in these graphs for above mentioned values of the order. Again, values of all passive components and gains are summarized in Table 3 shown above.

From magnitude responses in Fig. 9 and Fig. 10 can be seen that obtained measurement results (solid lines) are slightly different in comparison with simulation results (dashed lines). Differences at higher frequencies (around 8 MHz) are caused by bandwidth limitations of the used active elements and parasitic capacitance of the designed PCB and are not important in these cases. Other differences are given by inaccuracies of the gains and passive elements.
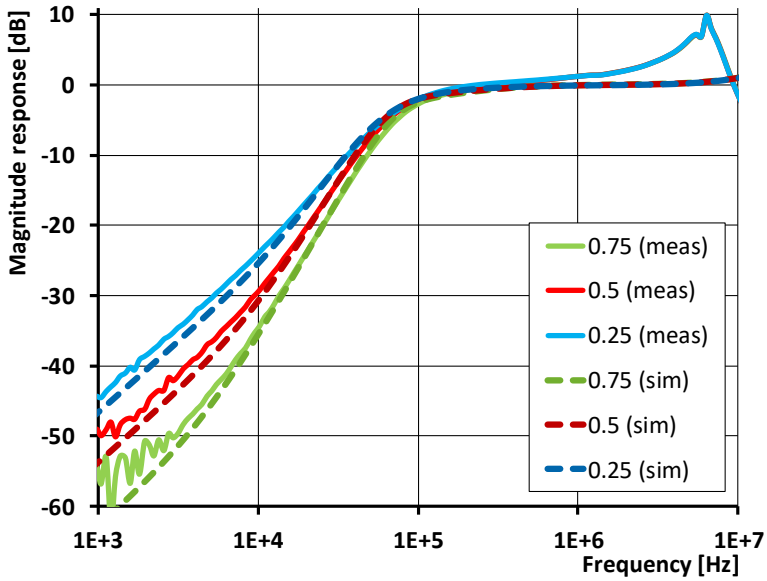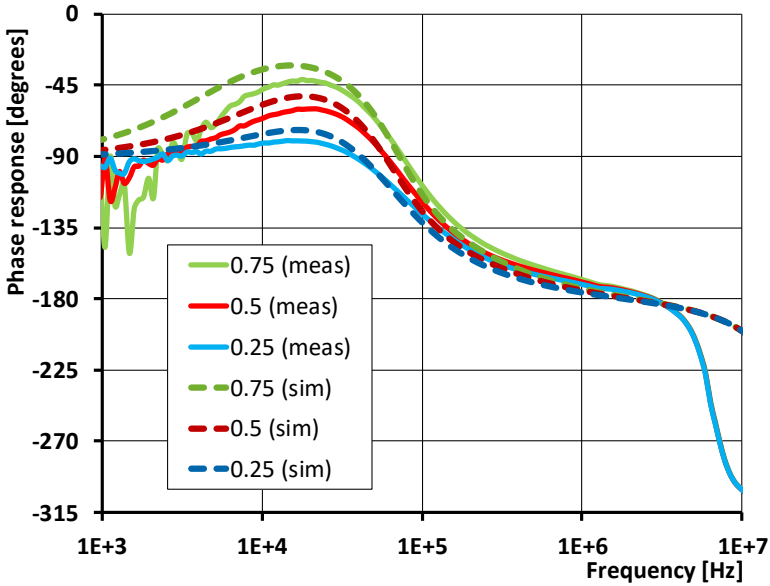

(a)
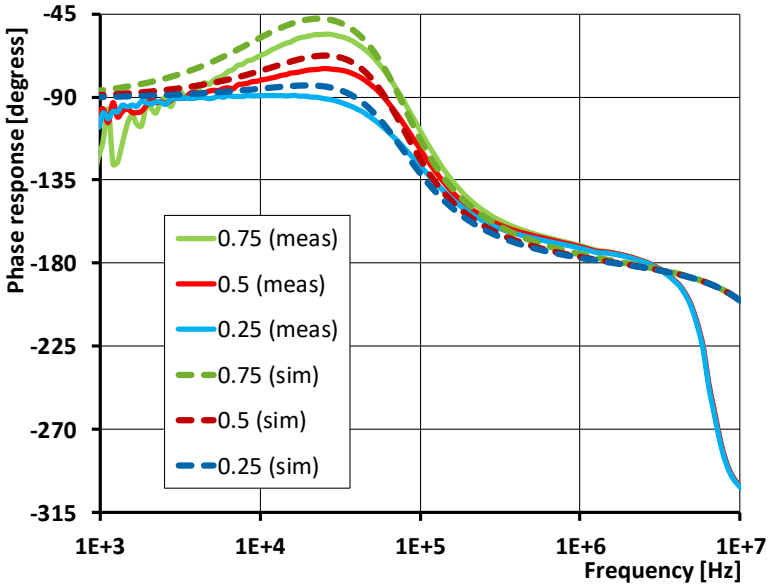
(b)

Fig. 9. Simulation (dashed lines) and measurement (solid lines) results of the FHPF for 1st approximation: (a) magnitude response, (b) phase response.


(a)

(b)

Fig. 10. Simulation (dashed lines) and measurement (solid lines) results of the FHPF for 2nd approximation: (a) magnitude response, (b) phase response.

### 5.3. *Control of the frequencies of both the FLPF and FHPF*

Magnitude and phase responses while electronically controlling the pole frequency of the FLPF, for used 2nd approximation as an example, are shown in Fig. 11 (a), (b). Chosen pole frequencies are: 33, 100 and 300 kHz and all other parameters are summarized in Table 4. A comparison of the measurement (solid lines) and simulation (dashed lines) results is performed also in this case.

From Fig. 11 (a) it is obvious that measurement and simulation results are very similar. However, results for filter with the pole frequency $f_{0\_LP} = 300$ kHz are affected by really small values of the $1/g_m$-s (see Table 4).

Figure 12 (a), (b) illustrates magnitude and phase response of the three selected values of the pole frequency of the FHPF (again the 2nd approximation is used as an example, all parameters are shown in Table 5). From Fig. 12 is obvious that obtained results are also in good agreement with theory. The bandwidth limitations of the used active elements can be seen at higher frequencies.
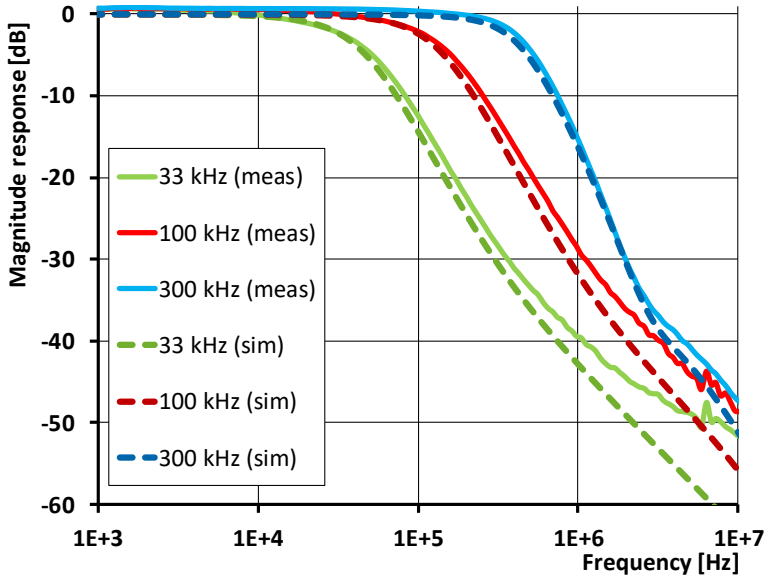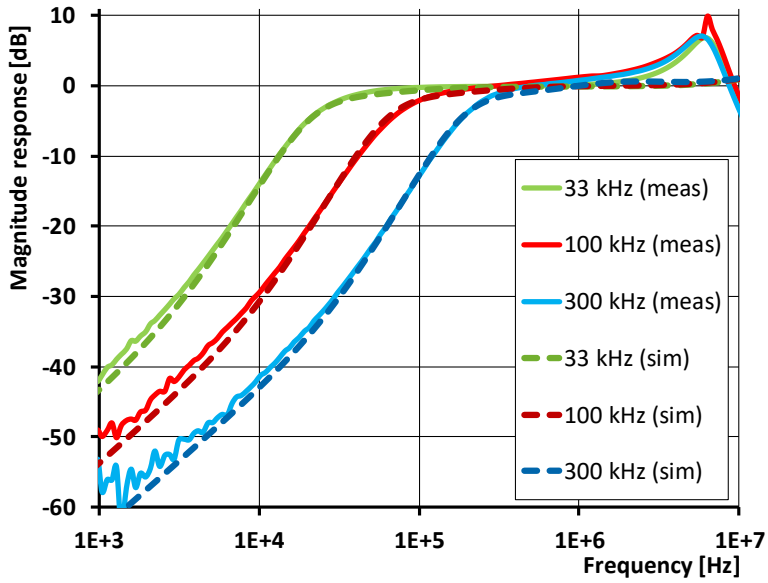
(a)
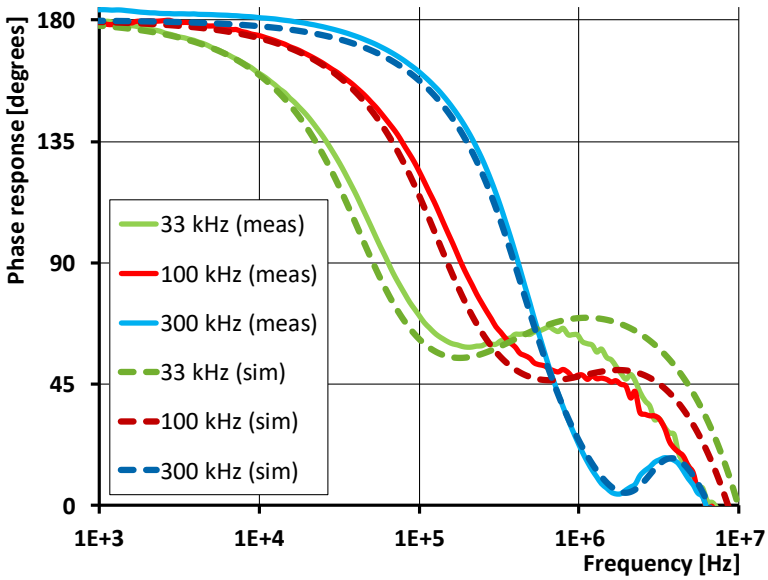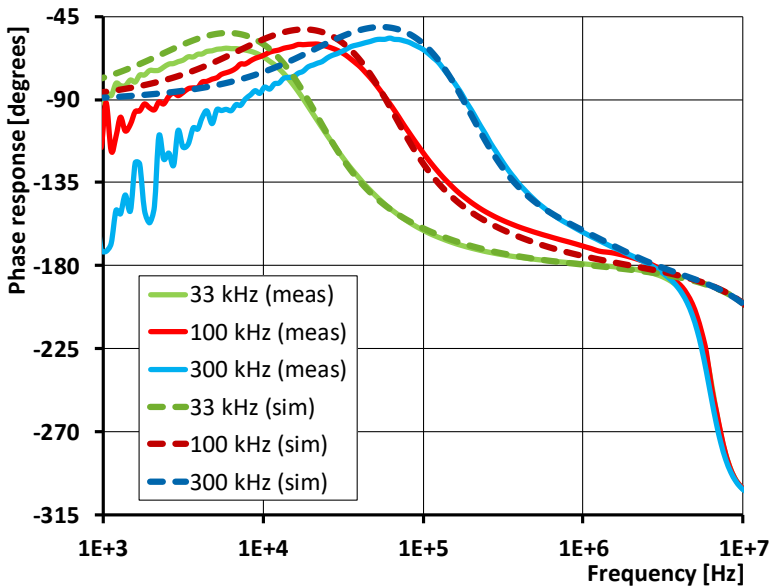

(b)

Fig. 11. Demonstration of the electronic control of the pole frequency of the FLPF for 2nd approximation with constant order equal to 1.5: (a) magnitude response, (b) phase response.

(a)

(b)

Fig. 12. Demonstration of the electronic control of the pole frequency of the FHPF for 2nd approximation with constant order 1.5: (a) magnitude response, (b) phase response.

5.4. *Summarization of the obtained results*

Table 6 and Table 7 summarize obtained values of the slope of attenuation of the transfer function of the FLPF and FHPF for three designed values of the order. A comparison of the values of the slope of attenuation of the filters for 1st and 2nd approximation is made. From obtained experimental results can be seen that values of the slope of attenuation are not far from the theoretical results. FLPF for 1st and 2nd approximation is performing very similarly. Bigger differences are seen between values of the slope of attenuation of the FHPF for 1st and 2nd approximation.

The obtained theoretical, simulated and measured results of the pole frequency while tuning of the FLPF and FHPF, for chosen 2nd approximation, are compared in Table 8 and Table 9. From obtained values of the pole frequency of the FLPF (Table 8) can be seen that measurement results are very close to the theory. The biggest difference between theoretical and measured values of the pole frequency of the FLPF is obvious for the highest configured pole frequency (300 kHz). It is caused by relative small value of the resistors R_1, R_2 and R_3. From measurement results of the frequency tuning of the FHPF (Table 9) is obvious that obtained values of the pole frequency are also very close to the theoretical assumptions.

Table 6. Comparison of the theoretical, simulated and measured values of slope of attenuation of the filter in FLPF configuration for pole frequency of the filter 100 kHz. Both 1st and 2nd approximation ($1^{st}/2^{nd}$ value if applicable).

	Order		
Slope of attenuation [dB/dec]	1.25	1.5	1.75
Theoretical	25.0	30.0	35.0
Simulated	22.7 / 24.2	29.8 / 31.6	36.3 / 36.9
Measured	23.9 / 24.2	30.0 / 29.8	35.3 / 35.2

Table 7. Comparison of the theoretical, simulated and measured values of slope of attenuation of the filter in FHPF configuration for pole frequency of the filter 100 kHz. Both 1st and 2nd approximation ($1^{st}/2^{nd}$ value if applicable).

	Order		
Slope of attenuation [dB/dec]	1.25	1.5	1.75
Theoretical	25.0	30.0	35.0
Simulated	25.7 / 24.3	31.5 / 31.0	36.7 / 35.6
Measured	22.8 / 24.7	29.5 / 31.5	34.9 / 35.9

Table 8. Comparison of the theoretical, simulated and measured values of the pole frequency of the filter in FLPF configuration for constant order of the filter 1.5. The 2nd approximation is used.

	Pole frequency [kHz]		
Theoretical	33.0	100.0	300.0
Simulated	35.9	112.1	383.5
Measured	33.1	108.0	398.1

Table 9. Comparison of the theoretical, simulated and measured values of the pole frequency of the filter in FHPF configuration for constant order of the filter 1.5. The 2nd approximation is used.

	Pole frequency [kHz]		
Theoretical	33.0	100.0	300.0
Simulated	27.3	81.4	227.2
Measured	27.0	95.5	289.8

6. Conclusion

Reconfiguration of the transfer function between particular solutions of FLPF and FHPF was proved to be applicable by the structure presented in this paper. Achieved results prove also possibility of electronic and mutually independent control of fractional-order and pole frequency by changing values of the parameters of the filter. Moreover, also electronic control of type of approximation was proven to be possible. Verification with the behavioral models is very useful because it helps to verify successfully the design correctness not only in PSpice simulations but also by measurements with real devices in laboratory experiments. The measured results in case of the electronic control of the order and also the pole frequency are in good agreement with theoretical expectations. Note that this paper is significantly extended version of paper published as Ref. 48.

References

1. M. Ortigueira, An Introduction to the fractional continuous-time linear systems: The 21st century systems, *IEEE Circuits and Systems Magazine* **8** (2008) 19–26.
2. A. S. Elwakil, Fractional-order circuits and systems: An emerging interdisciplinary research area, *IEEE Circuits and Systems Magazine* **10** (2010) 40–50.
3. T. Freeborn, A survey of fractional-order circuit models for biology and biomedicine, *IEEE Journal on Emerging and Selected Topics in Circuits and Systems* **3** (2013) 416–424.
4. A.S. Elwakil and B. Maundy, Extracting the Cole-Cole impedance model parameters without direct impedance measurement, *Electron. Lett.* **46** (2010) 1367–1368.

5. T. J. Freeeborn, A. Elwakil and B. Maundy, Electrode location impact on Cole-impedance parameters using magnitude-only measurements, *Proc. 59th IEEE Int. Midwest Symposium on Circuits and Systems* (UAE, Abu Dhabi, 2016), pp. 21–24.

6. J. Valsa, P. Dvorak and M. Friedel, Network model of CPE, *Radioengineering* **20** (2011) 619–626.

7. J. Valsa and J. Vlach, RC models of a constant phase element, *International Journal of Circuit Theory and Applications* **41** (2013) 59–67.

8. B. M. Vinagre, I. Podlubny, A. Hernandez and V. Feliu, Some approximations of fractional order operators used in control theory and applications, *Fractional Calculus & Applied Analysis* **3** (2000) 231–248.

9. J. Petrzela, T. Gotthans and Z. Hrubos, General review of the passive networks with fractional-order dynamics, *Proc. International Conference on Circuits, Systems, Control, Signals* (2012), pp. 172–177.

10. J. Petrzela, Analog continuous-time filtering extended to fractional-order network elements, *Proc. 36th Int. Conf. Telecommunications and Signal Processing TSP* (2013), pp. 417–421.

11. J. Petrzela, Fundamental Analog Cells for Fractional-Order Two-Port Synthesis, *Proc. 23rd Int. Conf. Radioelektronika* (2013), pp. 182–187.

12. J. Petrzela, A note on fractional-order two-terminal devices in filtering applications, *Proc. 24th Int. Conf. Radioelektronika* (2014), pp. 1–4.

13. M. Tripathy, D. Mondal, K. Biswas and S. Sen, Experimental studies on realization of fractional inductors and fractional-order bandpass filters, *International Journal of Circuit Theory and Applications* **43** (2015) 1183–1196.

14. I. Dimeas, G. Tsirimokou, C. Psychalinos and A. Elwakil, Realization of Fractional-Order Capacitor and Inductor Emulators Using Current Feedback Operational Amplifiers, *Proc. Int. Symposium on Nonlinear Theory and its Applications NOLTA* (China, Hong Kong, 2015), pp. 237–240.

15. G. Tsirimokou, C. Psychalinos, A. S. Elwakil and K. N. Salama, Experimental verification of on-chip CMOS fractional-order capacitor emulators, *Electronics Letters* **52** (2016) 1298–1300.

16. G. Tsirimokou, C. Psychalinos and A. S. Elwakil, Emulation of a constant phase element using operational transconductance amplifiers, *Analog Integrated Circuits and Signal Processing* **85** (2015) 413–423.

17. G. Tsirimokou, C. Laoudias and C. Psychalinos, 0.5-V fractional-order companding filters, *International Journal of Circuit Theory and Applications* **43** (2015) 1105–1126.

18. G. Tsirimokou and C. Psychalinos, Ultra-low voltage fractional-order circuits using current mirrors, *International Journal of Circuit Theory and Applications* **44** (2016) 109–126.

19. T. Freeborn, B. Maundy and A. Elwakil, Field programmable analogue array implementation of fractional step filters, *IET Circuits, Devices and Systems* **4** (2010) 514–524.

20. B. Maundy, A. Elwakil and T. Freeborn, On the practical realization of higher-order filters with fractional stepping, *Signal Processing* **91** (2011) 484–491.

21. R. Sotner, J. Jerabek, J. Petrzela and T. Dostal, Simple Approach for Synthesis of Fractional-Order Grounded Immittances Based on OTAs, *Proc. Int. Conf. Telecommunications and Signal Processing TSP* (2016), pp. 563–568.

22. R. Sotner, J. Jerabek, N. Herencsar, J. Petrzela, T. Dostal and K. Vrba, First-order adjustable transfer sections for synthesis suitable for special purposes in constant phase block approximation, *International Journal of Electronics and Communications* **69** (2015) 1334-1345.

23. M. Krishna, S. Das, K. Biswas and B. Goswami, Fabrication of a fractional order capacitor with desired specifications: a study on process identification and characterization, *IEEE Trans. Electron Devices* **58** (2011) 4067–4073.

24. A. M. Elshurafa, M. N. Almadhoun, K. N. Salama and H. N. Alshareef, Microscale electrostatic fractional capacitors using reduced graphene oxide percolated polymer composites, *Applied Physics Letters* **102** (2013) 232901–4.

25. A. Adhikary, M. Khanra, S. Sen and K. Biswas, Realization of carbon nanotube based electrochemical fractor, *Proc. IEEE Int. symposium on Circuits and Systems ISCAS* (Portugal, Lisbon, 2015), pp. 2329–2332.

26. P. Ushakov, A. Shadrin, D. Kubanek and J. Koton, Passive Fractional-Order Components Based On Resistive- Capacitive Circuits With Distributed Parameters, *Proc. 39th Int. Conf. Telecommunications and Signal Processing TSP* (2016), pp. 638–642.

27. P. Ahmadi, B. Maundy, A. Elwakil and L. Belostotski, High-quality factor asymmetric-slope band-pass filters: a fractional-order capacitor approach, *IET Circuits, Devices and Systems* **6** (2012) 187–197.

28. M. Tripathy, K. Biswas and S. Sen, A design example of a fractional-order Kerwin–Huelsman–Newcomb biquad filter with two fractional capacitors of different order, *Circuits Systems and Signal Processing* **32** (2013) 1523-1536.

29. A. Ali, A. Radwan and A. Soliman, Fractional order Butterworth filter: active and passive realizations, *IEEE Journal on Emerging and Selected Topics in Circuits and Systems* **3** (2013) 346–354.

30. A. Soltan, A. G. Radwan and A. M. Soliman, Fractional Order Sallen-Key and KHN filters: Stability and Poles Allocation, *Circuits Systems and Signal Processing* **34** (2015) 1461–1480.

31. T. Freeborn, B. Maundy and A. Elwakil, Toward the realization of fractional step filters, *Proc. IEEE International Symposium on Circuits and Systems ISCAS* (France, Paris, 2010), pp. 1037–1040.

32. B. Maundy, A. Elwakil and T. Freeborn, On the practical realization of higher-order filters with fractional stepping, *Signal Processing* **91** (2011) 484–491.

33. F. Khateb, D. Kubanek, G. Tsirimokou and C. Psychalinos, Fractional-order filters based on low-voltage DDCCs, *Microelectronics Journal* **50** (2016) 50–59.

34. G. Tsirimokou, C. Psychalinos and A. S. Elwakil, Fractional-order electronically controlled generalized filters, *Int. Journal of Circuit Theory and Applications* (2016). Online first, doi: 10.1002/cta.2250.

35. J. Dvorak, L. Langhammer, J. Jerabek, J. Koton, R. Sotner and J. Polak, Electronically Tunable Fractional-Order Low- Pass Filter with Current Followers, *Proc. 39th International Conference on Telecommunications and Signal Processing TSP* (2016), pp. 587–592.

36. D. Biolek, R. Senani, V. Biolkova and Z. Kolka, Active elements for analog signal processing: Classification, Review and New Proposals, *Radioengineering* **17** (2008) 15–32.

37. J. Jerabek, J. Koton, R. Sotner and K. Vrba, Adjustable band-pass filter with current active elements: two fully-differential and single-ended solutions, *Analog integrated circuits and signal processing* **74** (2013) 129–139.

38. G. E. Carlson and C. A. Halijak, Approximation of fractional capacitors $(1/s)^{\wedge}(1/n)$ by a regular Newton process, *IEEE Transactions on Circuit Theory* **11** (1964) 210–213.

39. K. Matsuda and H. Fujii, H$_\infty$–optimized wave-absorbing control: analytical and experimental results, *Journal of Guidance, Control, and Dynamics* **16** (1993) 1146–1153.

40. A. Oustaloup, *Systèmes Asservis Linéaires d'Ordre Fractionnaire: Théorie et Pratique* (Masson: Paris, 1983).

41. A. Oustalou, *La Dérivation Non Entière, Théorie, Synthèse et Applications* (Hermes Science Publications, Paris, 1995).

42. A. Oustaloup, F. Levron, B. Mathieu and F. Nanot, Frequency-band complex non integer differentiator: characterization and synthesis, *IEEE Transactions on Circuits and Systems – I: Fundamental Theory and Applications* **47** (2000) 25–39.

43. A. Djouambi, A. Charef and A. Besançon, Optimal approximation, simulation and analog realization of the fundamental fractional order transfer function, *International Journal of Applied Mathematics and Computer Science* **17** (2007) 455–462.

44. C. Gruau, D. Picart, R. Belmas, E. Bouton, F. Delmaire-Sizes, J. Sabatier and H. Trumel, Ignition of a confined high explosive under low velocity impact. *International Journal of Impact Engineering* **36** (2009) 537–550.

45. B. Krishna and K. Reddy, Active and passive realization of fractance device of order ½, *Active and Passive Electronic Components Hindawi Publishing Corporation* **2008** (2008) 1–5.

46. L. Kadlcik and P. Horsky, A Low-Dropout Voltage Regulator with a Fractional-Order Control, *Radioengineering* **25** (2016) 312–320.

47. J. Jerabek and K. VRBA, SIMO type low-input and high-output impedance current- mode universal filter employing three universal current conveyors, *AEU - International Journal of Electronics and Communications,* **64** (2010) 588–593.

48. J. Jerabek, R. Sotner, D. Kubanek, J. Dvorak, L. Langhammer, N. Herencsar and K. Vrba, Fractional-Order Low-Pass Filter with Electronically Adjustable Parameters, *Proc. Int. Conference on Telecommunications and Signal Processing* (Vienna, Austria, 2016), pp. 569-574.

49. J. Jerabek, R. Sotner, J. Dvorak, L. Langhammer, and J. Koton, Fractional-order high-pass Filter with electronically adjustable parameters, *Proc. 2016 International Conference on Applied Electronics (AE)* (Pilsen, Czech Republic, 2016), pp. 111-116.

50. Datasheet EL2082 (Elantec), *Current-mode multiplier* (intersil, rev. D, 1996). Available online at <http://www.intersil.com/content/dam/Intersil/documents/el20/el2082.pdf>.